DOI 10.5012/bkcs.2011.32.5.1579

The Preparation of Alumina Particles Wrapped in Few-layer Graphene Sheets and Their Application to Dye-sensitized Solar Cells

Kwang-Soon Ahn, Sang-Won Seo, Jeong-Hyun Park, Bong-Ki Min,† and Woo-Sik Jung*

School of Chemical Engineering, College of Engineering, Yeungnam University, Gyongsan 712-749, Korea
**E-mail: wsjung@yu.ac.kr*
†Center for Research Utilities, Yeungnam University, Gyongsan 712-749, Korea
Received December 2, 2010, Accepted March 21, 2011

Alumina particles wrapped in few-layer graphene sheets were prepared by calcining aluminum nitride powders under a mixed gas flow of carbon monoxide and argon. The graphene sheets were characterized by powder X-ray diffraction (XRD), Raman spectroscopy, electron energy loss spectroscopy, and high-resolution transmission electron microscopy. The few-layer graphene sheets, which wrapped around the alumina particles, did not exhibit any diffraction peaks in the XRD patterns but did show three characteristic bands (D, G, and 2D bands) in the Raman spectra. The dye-sensitized solar cell (DSSC) with the alumina particles wrapped in few-layer graphene sheets exhibited significantly improved overall energy-conversion efficiency, compared to conventional DSSC, due to longer electron lifetime.

Key Words : Graphene sheets, Aluminum nitride, Carbon monoxide, Dye-sensitized solar cell

Introduction

Since the first report on electrical properties of single layer graphene by Novoselov and Geim in 2004,[1] graphene, a one-atom-thick planar sheet of sp^2-bonded carbon atoms densely packed in a two-dimensional honeycomb crystal lattice, has attracted considerable interest because of its unique physical, chemical, and mechanical properties.[2-5] However, the preparation of graphene sheets remains challenging. The main preparation methods reported so far are micromechanical cleavage of bulk graphite,[1,2] graphite oxidation-exfoliation-reduction,[4-9] ultrahigh vacuum graphitization of silicon carbide,[10,11] plasma enhanced chemical vapor deposition using methane as the carbon source,[12] and substrate-free gas-phase synthesis using a microwave plasma reactor.[13] In recent years, we prepared graphene sheets by the reduction of CO by aluminum sulfide (Al_2S_3).[14,15]

In this present work, we show another method for synthesis of graphene sheets by using CO gas which is reduced by aluminum nitride (AlN) powders. The reaction of CO with AlN is the reverse reaction of the carbothermal reduction and nitridation (CRN) reaction of alumina (Al_2O_3). The CRN reaction is expressed as follows:

$$Al_2O_3(s) + 3C(s) + N_2(g) \rightarrow 2\ AlN(s) + 3\ CO(g) \qquad (1)$$

The CRN method is one of the most useful methods to synthesize AlN powders.[16] The graphene sheets prepared in this work were characterized by powder X-ray diffraction (XRD), Raman spectroscopy, electron energy loss spectroscopy (EELS), and high-resolution transmission electron microscopy (HRTEM). The characterization revealed few-layer graphene sheets wrapped around alumina particles, which were applied to dye-sensitized solar cells (DSSCs) based on mesoporous TiO_2 layers. DSSCs have been extensively studied as a low-cost alternative to commercial, silicon-based solar cells.[17,18] However, the DSSCs have yet to be improved and their major bottleneck is directly related to large recombination rate, because the mesoporous TiO_2 films composed of the nanoparticles smaller than 30 nm don't develop a depletion layer at the interface between the TiO_2 and electrolyte, leading to large back electron transfer.[19,20] It has recently been reported that the graphene in the mesoporous TiO_2 electrodes benefits the charge separation and reduces the recombination rate, because it is a zero band gap material with electrons acting massless relativistic particles, so it provides an excellent electrical pathway.[21,22]

Experimental Section

Preparation of Alumina Particles Wrapped in Graphene Sheets. The AlN powders were prepared by calcining a (hydroxo)(succinato)Al(III) complex at 1300 °C for 5 h under a flow of nitrogen.[23] The powders in an alumina crucible were set in an alumina tube with an inner diameter of 36 mm and heated at a rate of 5 °C/min to 1400 °C in a gas mixture of argon and 10 vol % CO (hereafter referred to as 10 vol % CO/Ar) at a flow rate of 200 mL/min. The as-synthesized products were characterized by powder XRD (PANalytical X'Pert PRO MPD X-ray diffractometer with Cu-Kα radiation operating at 40 kV and 30 mA). The carbon content in the products was determined by a CHN elemental analyzer (Flash 1112, Thermo Fischer Scientific). Raman spectra were measured using a home-built microRaman system. The incident laser light of a He-Ne laser (632.8 nm, 3 mW) was focused on the sample through an objective (×100, NA = 0.7). The Raman scattered light was collected by the same objective and sent to the spectrometer. The acquisition time of each spectrum was 1 min. A Cs-corrected

Hitachi HD-2700 scanning transmission electron microscope equipped with a Gatan Imaging Filter was used to measure the HRTEM images and EELS spectra.

DSSCs with the Alumina Particles Wrapped in Graphene Sheets. The graphene-TiO_2 composite mesoporous film was prepared by paint shaking and dispersing the alumina particles wrapped in graphene sheets (1 wt %) and commercial TiO_2 (P25) nanoparticles together in ethanol. The graphene-TiO_2 colloid was thoroughly dispersed using a conditioning mixer by adding ethyl cellulose as a binder and α-terpineol as a solvent for the graphene-TiO_2 paste, after which the mixture was concentrated using an evaporator. An 18 μm-thick, mesoporous graphene-TiO_2 layer was prepared by doctor-blading the graphene-TiO_2 paste on the fluorine-doped tin oxide (FTO) transparent conducting oxide (TCO), followed by calcination at 450 °C for 30 min. For comparison, an 18 μm-thick, mesoporous TiO_2 layer without the graphene sheets was also prepared. The photoanodes were immersed in ethanol solution of N3 dye overnight for dye-adsorption, rinsed with ethanol, and dried at 50 °C.

The DSSCs with and without the alumina particles wrapped in graphene sheets were prepared with a platinum counter electrode and an electrolyte composed of 0.6 M 3-hexyl-1,2-dimethyl imidazolium iodide, 0.05 M iodine, 0.05 M LiI, and 0.5 M 4-*tert*-butylpyridine in acetonitrile. The photovoltaic characteristics of the DSSCs were measured under 1 sunlight intensity (100 mW cm^{-2}, AM1.5) that was verified with an AIST-calibrated Si-solar cell (PEC-L11, Peccell Technologies, Inc.).

Results and Discussion

The black powders were obtained by calcining AlN powders (Figure 1(a)) at 1400 °C for 5 and 20 h under a flow of 10 vol% CO/Ar. The XRD pattern (Fig. 1(b)) of the sample obtained after 5 h (hereafter referred to as Sample A) exhibited weak diffraction peaks assigned to δ-Al_2O_3 (JCPDS Card No. 46-1131), together with diffraction peaks assigned to AlN (JCPDS Card No. 25-1133). In the XRD pattern (Fig. 1(c)) of the sample obtained after 20 h (hereafter referred to as Sample B), peaks assigned to AlN, δ-Al_2O_3, and α-Al_2O_3 (JCPDS Card No. 46-1212), were detected. The carbon content in Samples A and B was 2.7 and 5.2 weight%, respectively, indicating that the black color of the two samples was due to the carbonaceous material they contained. The observation of Al_2O_3 and carbon in the product powders indicated that the reverse reaction of Eq. (1) occurred at 1400 °C. We recently showed that the CRN reaction of Al_2O_3 under a mixed gas flow of CO and N_2 becomes more retarded with increasing CO content.[24] The retardation effect of CO on the CRN reaction indicated the occurrence of the reverse reaction of Eq. (1).

No diffraction peaks assigned to the carbonaceous material were detected, as shown in Figures 1(b) and (c). In order to identify the carbonaceous material, we measured the Raman spectra of the product powders. Raman spectroscopy is one of the most powerful characterization tools for carbonaceous

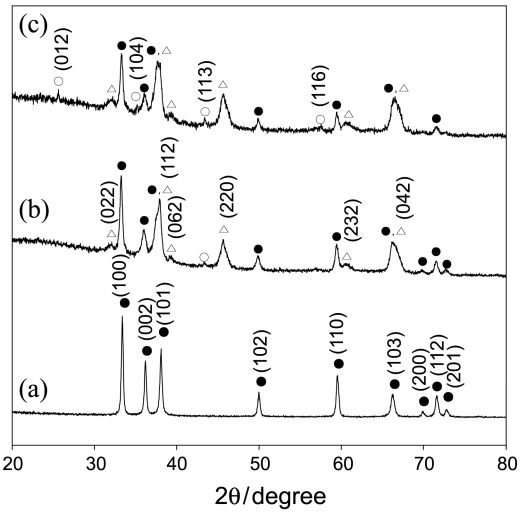

Figure 1. XRD patterns of powders obtained by the calcination of (a) AlN powder at 1400 °C for (b) 5 and (c) 20 h under a flow of 10 vol % CO/Ar. (●) AlN, (○) α-Al_2O_3, (△) δ-Al_2O_3.

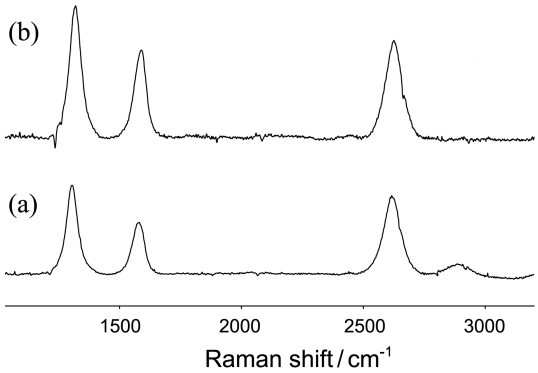

Figure 2. Raman spectra of powders obtained by calcination of AlN powder at 1400 °C for (a) 5 and (b) 20 h under a flow of 10 vol % CO/Ar.

materials such as two-dimensional graphene sheets and one-dimensional carbon nanotubes.[25] As shown in Figure 2, the Raman spectra of Samples A and B exhibited three characteristic bands of graphene sheets: D (at 1314 and 1317 cm^{-1} for Samples A and B, respectively), G (at 1588 cm^{-1} for both samples), and 2D (2614 cm^{-1} and 2624 cm^{-1} for Samples A and B, respectively). The weak and broad band at 2870 cm^{-1} in Figure 2(a) was assigned to the D + G combination band. In our previous study, the graphene sheets prepared by the reaction of CO with Al_2S_3 in the temperature range 800-1100 °C did not exhibit their characteristic XRD peaks but did show intense D, G, and 2D bands in the Raman spectra.[15] Therefore, the absence of any diffraction peaks assigned to the graphene sheets in Figures 1(b) and (c) was ascribed to the small number of graphene layers and/or the low crystallinity of the graphene sheets.[15] The D band is due to the breathing modes of sp^2 atoms in rings. In general, the D band, which has often been observed for graphene sheets prepared by chemical reactions,[26-28] is related to the occurrence of defects and structural disorder in graphene sheets.[25] The

G band corresponds to the E_{2g} phonon at the Brillouin zone center. The intensity ratio of the D band to the G band slightly decreased with increasing duration because of the reduced degree of defects and structural disorder in the graphene sheets.[29] The reduction was also indicated by the disappearance of the D + G combination band, which is induced by disorder,[29] as shown in Figure 2(b).

The band pattern of the Raman spectrum (Fig. 2(a)) of Sample A was similar to that of the graphene sheets (hereafter referred to as Sample C) that we previously obtained by calcination of Al_2S_3 at 1100 °C for 10 h under a flow of 10 vol % CO/Ar.[15] Comparing the positions of bands D, G, and 2D between Samples A and C, the position of the D band was similar in both samples, but the position of the G band was blue-shifted by ~17 cm^{-1}, while the position of the 2D band was red-shifted by ~20 cm^{-1}. The origin of the blue shift of the G band remains unclear but may have originated from the strain effect caused by the interaction between Al_2O_3 and graphene sheets. Wang *et al.* investigated the effect of substrates on the Raman spectrum of monolayer graphene.[30] The positions of the G and 2D bands were negligibly affected by substrates for the graphene prepared by mechanically cleavage of graphite, but were significantly blue-shifted for the epitaxially grown graphene on SiC.[30] They interpreted the blue shift in terms of the strain effect caused by the covalent bonding between SiC substrate and graphene. On the other hand, the red shift of the 2D band may be explained by a combination of effects caused by the strain and layer number. Considering that the position of the 2D band is red-shifted with decreasing number of layers of graphene sheets,[25] and given the very few layers in Samples A and B (see below), the red shift of the 2D band indicates that the strain effect may be overwhelmed by the effect of the layer number.

The graphene sheets in Sample B were characterized by HRTEM, operated at 80 kV. We previously reported that the graphene sheets obtained by the reaction of Al_2S_3 with CO were silk-like,[14,15] but those in Sample B were not. Four parallel dark fringes were observed at the edge of the Sample B particles, as shown in Figure 3(a). The spacing between the neighboring fringes was 0.34 nm, which was consistent with the spacing between the (002) planes of graphite. The EELS spectra in the carbon K-edge were also measured to ensure that the fringes were derived from graphene sheets. EELS is a powerful method to reveal the detailed structures and has been used largely to research amorphous and nanocrystalline carbon films.[31] As shown in Figure 3(b), the EELS spectrum for the fringes (spot ⓐ in Fig. 3(a)) showed the feature of a graphite EELS spectrum in the carbon K-edge region. The peaks at 287 and 294 eV correspond to transitions from the 1s to the π* and σ* states, respectively. The EELS spectrum for the upper surface (spot ⓑ in Fig. 3(a)) also exhibited the feature of a graphite EELS spectrum. The EELS spectra of Figure 3(b) indicated that few-layer graphene sheets wrapped around alumina particles. This wrapping may induce an interaction between the graphene sheets and alumina that causes the blue shift of the G band in the Raman spectrum.[30]

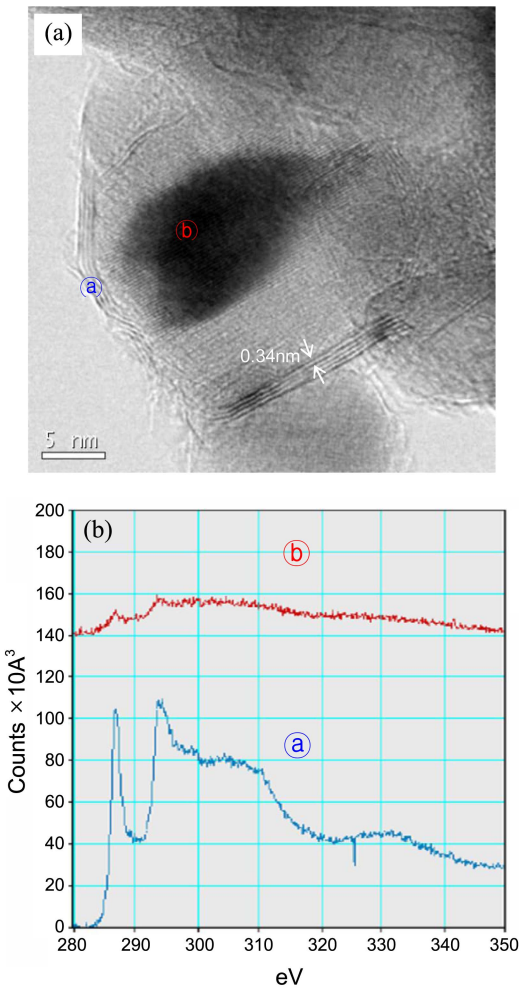

Figure 3. HRTEM image and EELS spectra of the powder obtained by calcination of AlN powder at 1400 °C for 20 h under a flow of 10 vol % CO/Ar.

The graphene sheets were formed by the reaction of CO with AlN in the reverse reaction of Eq. (1), in which CO is reduced to gaseous carbon, which subsequently crystallized in the graphene sheets, while AlN was converted to δ-Al_2O_3 and subsequently transformed into α-Al_2O_3. Incomplete conversion of AlN to Al_2O_3 in this study was attributed to the wrapping of graphene sheets, which hindered the diffusion of CO into the inner side of the AlN particles. In our previous investigation on the reduction of CO by Al_2S_3,[15] Al_2S_3 was completely converted to Al_2O_3 at 1400 °C due to the absence of any wrapping of the graphene sheets.

Figure 4 shows the photocurrent-voltage curves of the DSSCs without and with the alumina particles wrapped in few-layer graphene sheets. The DSSC with the graphene-TiO_2 composite electrode exhibited an 11% increase in higher overall energy conversion efficiency from 4.6 to 5.1%. The amount of the dye adsorbed in the 1 wt % graphene-TiO_2 film was slightly lower than that of the TiO_2 film. The graphene-incorporated TiO_2 films could, however, significantly enhance the electron lifetime, the details of which are described elsewhere.[32] Therefore, the significantly improved

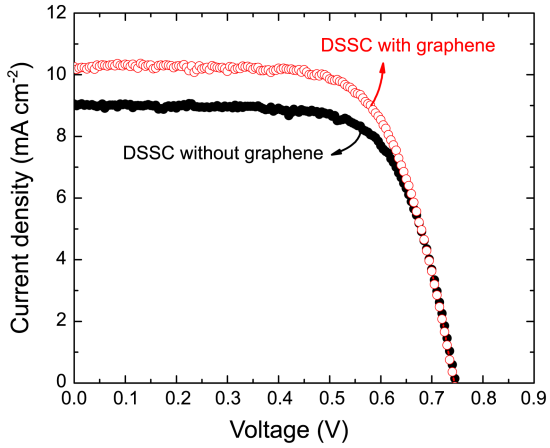

Figure 4. Photocurrent-voltage curves of the DSSCs with and without the alumina particles wrapped in graphene sheets. The active area was 0.24 cm^2.

cell performance of the DSSC with the graphene-TiO_2 composite electrode can be attributed to the reduced recombination rate caused by the longer electron lifetime.

Conclusions

This work has presented a method for the synthesis of alumina particles wrapped in few-layer graphene sheets by the reduction of CO. The CO was reduced to gaseous carbon by the reaction of AlN, which is the reverse reaction of the CRN reaction of alumina. The gaseous carbon crystallized in the graphene sheets. Few-layer graphene sheets, which wrapped around alumina particles, did not exhibit diffraction peaks in the XRD patterns but did show three characteristic D, G, and 2D bands in the Raman spectra. The positions of the G and 2D bands were different from those of the freestanding graphene sheets. The DSSC using TiO_2 nanoparticles mixed with alumina particles wrapped in few-layer graphene sheets exhibited significantly improved energy conversion efficiency, compared to the conventional DSSC, due to the reduced recombination rate caused by the enhanced electron lifetime.

Acknowledgments. This work is supported by the Ministry of Education, Science & Technology (MEST) and the National Research Foundation of Korea (NRF) under a "Human Resource Development Center for Economic Region Leading Industry" Project. One of the authors (WSJ) is grateful to Professor Bongsoo Kim, KAIST, Korea, for measuring the Raman spectra.

References

1. Novoselov, K. S.; Geim, A. K.; Morozov, S. V.; Jiang, D.; Zhang, Y.; Dubonos, S. V.; Grigorieva, I. V.; Firsov, A. A. *Science* **2004**, *306*, 666.
2. Novoselov, K. S.; Geim, A. K.; Morozov, S. V.; Jiang, D.; Katsnelson, M. I.; Grigorieva, I. V.; Dubonos, S. V.; Firsov, A. A. *Nature* **2005**, *438*, 197.
3. Katsnelson, M. I. *Materialstoday* **2007**, *10*, 20.
4. Stankovich, S.; Dikin, D. A.; Dommett, G. H. B.; Kohlhaas, K. M.; Zimney, E. J.; Stach, E. A.; Piner, R. D.; Nguyen, S. T.; Ruoff, R. S. *Nature* **2006**, *442*, 282.
5. Gómez-Navarro, C.; Burghard, M.; Kern, K. *Nano Lett.* **2008**, *8*, 2045.
6. Stankovich, S.; Piner, R. D.; Chen, X. Q.; Wu, N. Q.; Nguyen, S. T.; Ruoff, R. S. *J. Mater. Chem.* **2006**, *16*, 155.
7. Stankovich, S.; Dikin, D. A.; Piner, R. D.; Kohlhaas, K. A.; Kleinhammes, A.; Jia, Y.; Wu, Y.; Nguyen, S. T.; Ruoff, R. S. *Carbon* **2007**, *45*, 1558.
8. Wang, G.; Yang, J.; Park, J.; Gou, X.; Wang, B.; Liu, H.; Yao, J. *J. Phys. Chem. C* **2008**, *112*, 8192.
9. Kudin, K. N.; Ozbas, B.; Schiepp, H. C.; Pruïhomme, R. K.; Aksay, I. A.; Car, R. *Nano Lett.* **2008**, *8*, 36.
10. Berger, C.; Song, Z.; Li, T.; Li, X.; Ogbazghi, A. Y.; Feng, R.; Dai, Z.; Marchenkov, A. N.; Conrad, E. H.; First, P. N.; De Heer, W. A. *J. Phys. Chem. B* **2004**, *108*, 19912.
11. Ohta, T.; Bostwick, A.; Seyller, T.; Horn, K.; Rotenberg, E. *Science* **2006**, *313*, 951.
12. Wang, J. J.; Zhu, M. Y.; Outlaw, R. A.; Zhao, X.; Manos, D. M.; Holloway, B. C. *Appl. Phys. Lett.* **2004**, *85*, 1265.
13. Dato, A.; Radmilovic, V.; Lee, Z.; Phillips, J.; Frenklach, M. *Nano Lett.* **2008**, *8*, 2012.
14. Kim, C.-D.; Min, B.-K.; Jung, W.-S. *Carbon* **2009**, *47*, 1610.
15. Yoon, I.; Kim, C.-D.; Min, B.-K.; Kim, Y.-K.; Kim, B.; Jung, W.-S. *Bull. Korean Chem. Soc.* **2009**, *30*, 3045.
16. Selvadruray, G.; Sheet, L. *Mater. Sci. Technol.* **1993**, *9*, 463.
17. O'Regan, B.; Grätzel, M. *Nature* **1991**, *353*, 737.
18. Kang, S.-H.; Choi, S.-H.; Kang, M.-S.; Kim, J.-Y.; Kim, H.-S.; Hyeon, T.; Sung, Y.-E. *Adv. Mater.* **2008**, *20*, 54.
19. Ahn, K.-S.; Kang, M.-S.; Lee, J.-K.; Shin, B.-C.; Lee, J.-W. *Appl. Phys. Lett.* **2006**, *89*, 013103.
20. Archer, M. D.; Nozik, A. J. *Nanostructured and Photoelectro-Chemical Systems for Solar Photon Conversion*; Imperial College Press: Singapore, 2008.
21. Sun, S.; Gao, L.; Liu, Y. *Appl. Phys. Lett.* **2010**, *96*, 083113.
22. Yang, N.; Zhai, J.; Wang, D.; Chen, Y.; Jiang, L. *ACS Nano* **2010**, *4*, 887.
23. Jung, W.-S. *Bull. Korean Chem. Soc.* **2009**, *30*, 1563.
24. Joo, H. Y.; Jung, W.-S. *J. Mater. Proc. Technol.* **2008**, *204*, 498.
25. Ferrari, A. C. *Solid State Commun.* **2007**, *143*, 47.
26. Wang, J. J.; Zhu, M. Y.; Outlaw, R. A.; Zhao, X.; Manos, D. M.; Holloway, B. C.; Mammana, V. P. *Appl. Phys. Lett.* **2004**, *85*, 1265.
27. Dato, A.; Radmilovic, V.; Lee, Z.; Phillips. J.; Frenklach, M. *Nano Lett.* **2008**, *8*, 2012.
28. Wang, G.; Yang, J.; Park, J.; Gou, X.; Wang, B.; Liu, H.; Yao, J. *J. Phys. Chem. C* **2008**, *112*, 8192.
29. Pimenta, M. A.; Dresselhaus , G.; Dresselhaus, M. S.; Cançado, L. G.; Jori, A.; Saito, R. *Phys. Chem. Chem. Phys.* **2007**, *9*, 1276.
30. Wang, Y. Y.; Ni, Z. H.; Yu, T.; Shen, Z. X.; Wang, H. M.; Wu, Y. H.; Chen, W.; Wee, A. T. S. *J. Phys. Chem. C* **2008**, *112*, 10637.
31. Chu, P. K.; Li, L. *Mater. Chem. Phys.* **2006**, *96*, 253.
32. Park, J.-H.; Seo, S.-W.; Kim, J.-H.; Choi, C.-J.; Kim, H.-S.; Lee, D. K.; Jung, W.-S.; Ahn, K.-S. *Mol. Cryst. Liq. Cryst.* **2011**, in press.